AGU PUBLICATIONS

Geophysical Research Letters

RESEARCH LETTER
10.1002/2016GL067770

Key Points:
- Wind speed is a major driver of rain-aerosol relationships over the midlatitude oceans
- Wind speed mitigates the negative rain-aerosol relationships caused by wet scavenging
- Role of wind speed is larger than relative humidity

Supporting Information:
- Supporting Information S1

Correspondence to:
L. M. Russell,
lmrussell@ucsd.edu

Citation:
Yang, Y., L. M. Russell, S. Lou, Y. Liu, B. Singh, and S. J. Ghan (2016), Rain-aerosol relationships influenced by wind speed, *Geophys. Res. Lett.*, *43*, 2267–2274, doi:10.1002/2016GL067770.

Received 12 JAN 2016
Accepted 15 FEB 2016
Accepted article online 20 FEB 2016
Published online 8 MAR 2016

Rain-aerosol relationships influenced by wind speed

Yang Yang[1], Lynn M. Russell[1], Sijia Lou[1], Ying Liu[2], Balwinder Singh[2], and Steven J. Ghan[2]

[1]Scripps Institution of Oceanography, University of California, San Diego, La Jolla, California, USA, [2]Atmospheric Science and Global Change Division, Pacific Northwest National Laboratory, Richland, Washington, USA

Abstract Aerosol optical depth (AOD) has been shown to correlate with precipitation rate (R) in recent studies. The R-AOD relationships over oceans are examined in this study using 150 year simulations with the Community Earth System Model. Through partial correlation analysis, with the influence of 10 m wind speed removed, R-AOD relationships exert a change from positive to negative over the midlatitude oceans, indicating that wind speed makes a large contribution to the relationships by changing the sea-salt emissions. A simulation with prescribed sea-salt emissions shows that wind speed leads to increasing R by +0.99 mm d^{-1} averaged globally, offsetting 64% of the wet scavenging-induced decrease between polluted and clean conditions, defined according to percentiles of AOD. These demonstrate that wind speed is one of the major drivers of R-AOD relationships. Relative humidity at 915 hPa can also result in the positive relationships; however, its role is smaller than that of wind speed.

1. Introduction

Aerosols could be an important agent for perturbing both the Earth's radiative balance and atmospheric hydrological cycle. Aerosols can influence cloud microphysical processes, amount, and precipitation efficiency by serving as cloud condensation nuclei (CCN) [*Twomey*, 1977; *Albrecht*, 1989; *Lohmann and Feichter*, 2005]. However, these effects are nonlinear and highly uncertain, and dynamical factors make it difficult to identify comparable precipitation events. At present, it is difficult to establish systemically aerosol-cloud-precipitation relationships [*Stevens and Feingold*, 2009].

The dynamics of clouds and precipitation are driven by the thermodynamic trade-offs of latent and sensible heat for moist air as well as other meteorological factors, which often covary with each other as well as with aerosol amount. *Mauger and Norris* [2007], *Loeb and Schuster* [2008], and *Grandey et al.* [2013a] found that large-scale meteorological situations and synoptic systems lead to the covariation of aerosols and cloud fraction and thereby influence the apparent relationships between satellite-retrieved cloud fraction and aerosol optical depth (AOD).

Cloud fraction normally increases with relative humidity. Hygroscopic aerosols swell at high relative humidity, leading to an increase in AOD. Many previous observational and modeling studies reported that the major contribution to the positive relationships between AOD and cloud fraction is attributed to the covariation effect from relative humidity [*Quaas et al.*, 2010; *Chand et al.*, 2012; *Grandey et al.*, 2013b]. *Boucher and Quaas* [2013] reported that relative humidity has important influences on precipitation-AOD relationships. *Grandey et al.* [2014] also found that without wet removal of aerosols, correlations between AOD and precipitation rate are positive over almost all of the world. These positive correlations are partially due to covariation of aerosol and precipitation with relative humidity. However, in their study, even after the role of relative humidity is excluded, a positive relationship between precipitation rate and AOD remained.

Wind speed is also one of the most important factors that influence relationships between clouds, precipitation, and aerosols. Increasing wind speeds lead to increasing emissions of sea salt, which contributes the most to the AOD in clean marine air [*Haywood et al.*, 1999; *Mulcahy et al.*, 2008]. Winds, clouds, and precipitation are simultaneously symptomatic of meteorological conditions. Changes in winds can also influence moist transport into the cloud. These effects link winds to clouds and precipitation. Using satellite retrieved together with reanalysis data from the European Center for Medium Range Weather Forecasts (ECMWF) for years from 2003 to 2008, *Engström and Ekman* [2010] found that the correlation between AOD and cloud fraction was strongly influenced by 10 m wind speed. However, none of the previous studies has examined the contribution of wind speed to precipitation and aerosol relationships.

Previous studies have examined correlations between aerosols and clouds and between aerosols and precipitation through ground-based, aircraft, satellite observations and model simulations. Higher aerosol particle concentrations typically produce smaller cloud droplets, which decrease precipitation efficiency and could thereby prolong cloud lifetime [*Albrecht*, 1989]. Numerous studies using satellite data reported positive cloud fraction-AOD relationships that might result from aerosol-cloud interactions [*Kaufman et al*., 2005; *Koren et al*., 2005]. Absorbing aerosol can decrease cloud fraction through absorbing solar radiation, local heating, and evaporating cloud droplets [*Ackerman*, 2000]. Increases in CCN concentrations in aerosol-limited clouds also favor the condensation of supersaturated vapor and release of additional latent heat, which could invigorate water and mixed phase clouds [*Rosenfeld et al*., 2008; *Koren et al*., 2014]. *Koren et al*. [2012] found positive rain-AOD relationships in the tropics, subtropics, and midlatitudes in June–August 2007. They suggested that increasing aerosol concentration intensifies the rain rate.

Aerosols interact with clouds two ways. Aerosols impact clouds and precipitation, and clouds and precipitation can influence aerosols through wet scavenging processes [*Quaas et al*., 2010; *Grandey et al*., 2013b, 2014; *Gryspeerdt et al*., 2015]. *Grandey et al*. [2013b] found that wet scavenging by convective precipitation induces a strong negative cloud fraction-AOD correlation over the tropics through 1 year the global aerosol-climate model ECHAM-HAM model simulations. In *Grandey et al*. [2014], they further showed that wet scavenging also causes a strong negative rain rate-AOD correlation in the tropical and midlatitude oceans. Inside cloud droplets, sulfate mass is formed through aqueous chemistry, which leads to increases in AOD [*Su et al*., 2008]. *Koren et al*. [2007] reported increases in AOD due to aerosol growth hygroscopically around the clouds.

We present here an investigation of the impacts of wind speed on relationships between precipitation and aerosols based on a set of two 150 year simulations in preindustrial conditions using the Community Earth System Model (CESM) and comparisons to satellite-retrieved and reanalysis data. We quantify the contribution of wind speed to the relationships between precipitation rate and AOD through correlation analysis and a sensitivity simulation with prescribed sea-salt emissions. We also compare its contribution with those from other factors, such as wet scavenging and relative humidity.

2. Method

The model used here is the Community Earth System Model (CESM), which includes components from the Earth's atmosphere, ocean, land, land ice, and sea ice [*Hurrell et al*., 2013]. The atmosphere component used here is Version 5 of the Community Atmosphere Model (CAM5), which was run with a horizontal resolution of 1.9° latitude by 2.5° longitude and 30 vertical layers from the surface to about 2.3 hPa. The ocean component used here is a three-dimensional active model, the Parallel Ocean Program version 2 [*Smith et al*., 2010]. The modal aerosol module in the CESM-CAM5 simulates most aerosol species (sea salt, dust, sulfate, black carbon, primary organic matter, and secondary organic aerosol) in three modes [*Liu et al*., 2012]. Aerosol optical properties are parameterized according to *Ghan and Zaveri* [2007]. Activation of cloud droplets occurs on a multimodal lognormal aerosol size distribution based on the scheme of *Abdul-Razzak and Ghan* [2000]. The model physically treats the aerosol effects on stratiform cloud microphysics using physically based parameterizations [*Morrison and Gettelman*, 2008; *Gettelman et al*., 2010]. However, aerosol effects on convective clouds are neglected in the model. Aerosol wet scavenging is treated for both stratiform and convective clouds. The emissions of sea-salt particles with diameter $<$2.8 μm are parameterized in terms of 10 m wind speed and sea surface temperature [*Mårtensson et al*., 2003]. For diameters $>$2.8 μm, the emissions depend only on 10 m wind speed [*Monahan et al*., 1986].

To identify the contribution of wind speed to the relationships between aerosols and precipitation, two 150 year simulations at preindustrial conditions were performed: a control simulation, referred to as IRUN, with interactive sea-salt emissions, and a sensitivity simulation, referred to as ERUN, with prescribed sea-salt emissions. The emissions of sea-salt aerosol particles used in the ERUN simulation are interpolated in time between the 12 monthly mean values derived from the climatology of the 150 year IRUN simulation. By prescribing sea-salt emissions, the contribution of wind speed to the covariation of R and AOD is almost removed. Changes in sea surface temperature also affect emissions of sea-salt particles with diameter $<$ 2.8 μm, but the relatively small magnitude of these changes is unlikely to produce changes in our results. All anthropogenic and biomass burning emissions used in this study are fixed at 1850 levels to focus on the roles of wind-related sea-salt emissions. The model archived both monthly and daily data.

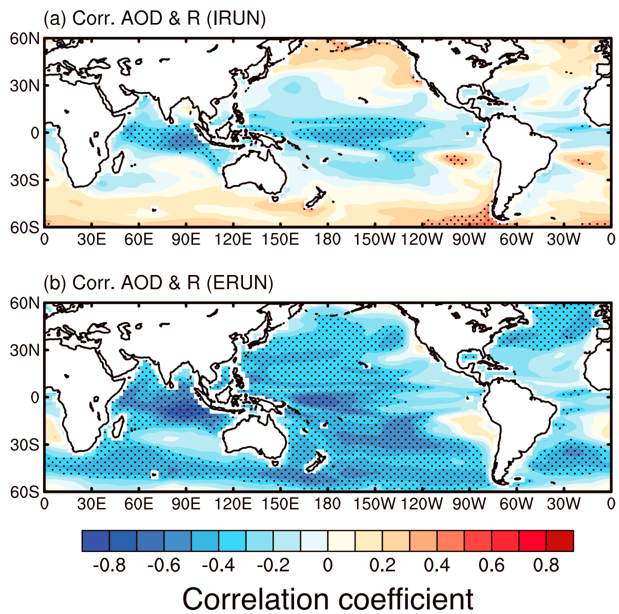

Figure 1. Total correlation coefficients between aerosol optical depth (AOD) and precipitation rate (*R*) for (a) IRUN and (b) ERUN simulations. The dotted areas indicate statistical significance with 95% confidence from a two-tailed Student's *t* test.

Results from these two simulations have been used to investigate the impacts of natural aerosol emissions and concentrations on variations of cloud radiative effects. Only ocean regions between 60°S and 60°N are analyzed in this study.

To examine the relationships between precipitation rate and aerosols, linear correlation coefficients between precipitation rate (*R*) and AOD are calculated for each grid box using monthly anomaly data from the 150 year IRUN and ERUN simulations. In addition to the total correlation, the partial correlation between *R* and AOD was also examined. The partial correlation measures the relationship between two variables, *R* and AOD, in this study, while taking away the effects of another variable, or several other variables, on this relationship [*Hazewinkel*, 2002]. This method has been used in many previous studies in examining the aerosol-cloud-precipitation relationships [*Engström and Ekman*, 2010; *Gryspeerdt et al.*, 2014]. We selected 10 m wind speed (U10) and relative humidity (RH) at 915 hPa as the controlling variables in partial correlation to compare the contributions of the wind speed and relative humidity to the relationships between *R* and AOD. Nine hundred fifteen hectopascal is chosen because this level is near the typical low cloud bases, and therefore, the impact of changes in aerosols will be relevant for the clouds and precipitation [*Lee et al.*, 2012].

To verify the covariation of *R* and AOD with wind speed, simulated correlations are compared with those calculated from satellite-retrieved and reanalysis data. Satellite-retrieved AODs are from Moderate Resolution Imaging Spectroradiometer. Wind speeds are derived from the ECMWF ERA-Interim reanalysis. *R* data are from CPC Merged Analysis of Precipitation (CMAP) data set. All data cover the years from 2001 to 2014.

To quantify the differences in *R* in different AOD conditions, we define the polluted and clean conditions categorized by the 67th and 33rd percentiles of AOD for each grid box and simulations following *Koren et al.* [2012]. Then the differences in *R* are calculated using the mean *R* for polluted and clean conditions.

3. Results

To examine the relationships between *R* and AOD, Figure 1a shows total correlation coefficients between *R* and AOD for the IRUN simulation. Statistically significant negative correlations are found in the tropical band between 20°S and 20°N, whereas insignificant positive correlations of AOD with *R* are simulated over the midlatitude oceans. This spatial pattern is identical to the findings in *Boucher and Quaas* [2013], which were conducted with a different model (ECHAM5-HAM). The area-weighted mean correlation coefficients are +0.11, −0.15, and +0.12 over the southern midlatitude (60–30°S), tropical (30°S–30°N), and northern midlatitude (30–60°N) bands, respectively (Table 1). The strong negative correlations between *R* and AOD and over the tropics result from the wet scavenging of aerosols, while positive values in the midlatitude are likely due to covariation with meteorological factors, such as relative humidity [*Grandey et al.*, 2014]. Averaged globally (60°S–60°N), there is no statistically significant correlation of *R* to AOD, with a correlation coefficient of −0.04.

To assess the effect of wind speed on the relationships between *R* and AOD, Figure 1b presents the total correlation coefficients between *R* and AOD for the ERUN simulation, which mitigates the role of wind speed on the relationships between precipitation and aerosols. In the ERUN simulation, the sea-salt emissions are interpolated with monthly climatological mean values derived from the IRUN simulation, and consequently,

Table 1. Area-Weighted Mean Correlation Coefficients Between Aerosol Optical Depth (AOD) and Precipitation Rate (*R*), and Composite Differences in *R* Between Polluted and Clean Conditions (unit: mm d^{-1}) Over the Southern Midlatitude (SL, 60°–30°S), Tropical (TR, 30°S–30°N), Northern Midlatitude (SL, 30°–60°N) Bands, and Globally (60°S–60°N)[a]

	Correlations AOD and *R*				Differences *R*			
Simulation	SL	TR	NL	Global	SL	TR	NL	Global
IRUN	+0.11	-0.15	+0.12	-0.04	+0.20	-1.13	+0.38	-0.56
ERUN	-0.34	-0.32	-0.28	-0.32	-0.81	-2.00	-1.11	-1.55
IRUN-ERUN	+0.45	+0.17	+0.40	+0.28	+1.01	+0.87	+1.49	+0.99

[a]Only ocean areas are considered.

the contribution of wind speed submonthly and interannual variability is removed. It is clear that the *R*-AOD relationships are significantly negative over almost all of the world for the ERUN simulation, in contrast to the positive relationships over the midlatitude oceans for the IRUN simulation. Averaged globally, the area-weighted mean correlation coefficient is −0.32 for ERUN. Negative relationships between *R* and AOD are mainly due to wet scavenging, as we show the impact of aerosol-cloud interactions is small in the following analysis. Comparing the correlation coefficients between IRUN and ERUN suggests that variations in wind speed lead to the positive relationships between *R* and AOD, with increases in correlation coefficients of +0.45, +0.17, and +0.40 over the southern midlatitude, tropical, and northern midlatitude bands, respectively (Table 1). The global area-weighted mean correlation coefficient increases by +0.28 resulting from the covariation effect of wind speed, which almost offsets the negative correlation coefficient of −0.32 caused by wet scavenging. This indicates that wind speed-driven emissions have a great influence on the *R*-AOD relationships.

To further examine the influence of wind speed and compare this effect with that of RH, Figure 2 shows the partial correlation coefficients and the differences between the total and partial correlations explained by U10 and RH at 915 hPa, respectively, for the IRUN simulation. Without the influence of U10, the relationships between *R* and AOD change from positive to negative over the midlatitude oceans (Figure 2a). Averaged globally, the area-weighted mean partial correlation coefficient is −0.16, which is a large increase in magnitude compared to the total correlation coefficient of −0.04. The largest differences between the total and partial correlation explained by U10 are located over the midlatitude oceans, where U10 leads to large

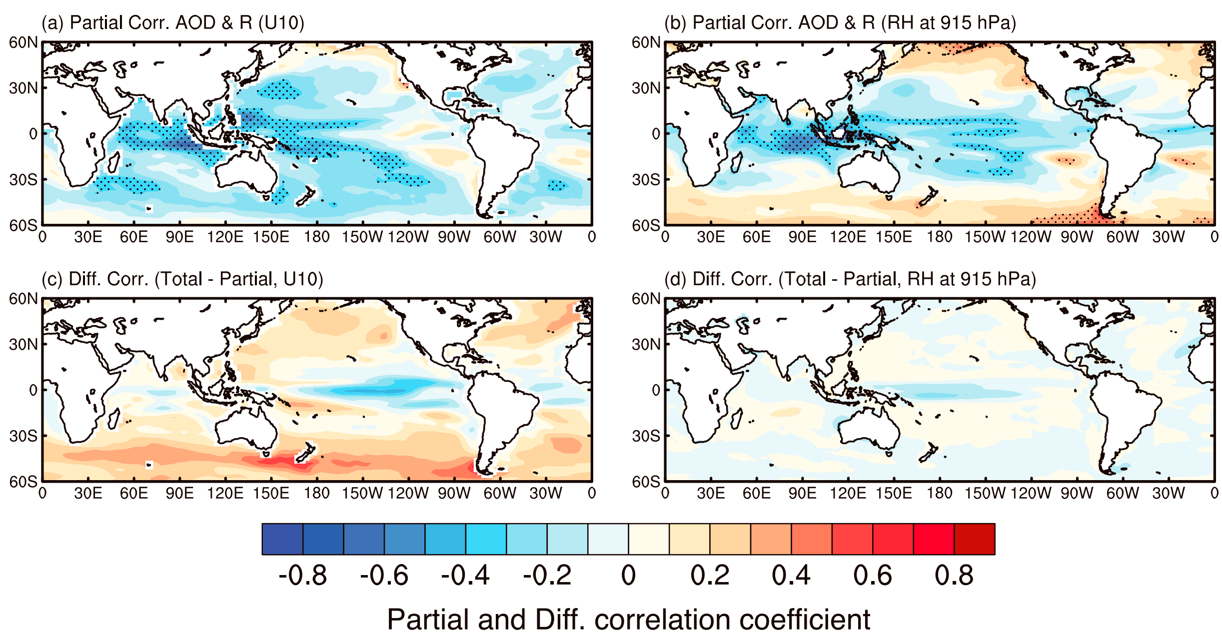

Figure 2. Partial correlation coefficients between AOD and *R* without influences of (a) 10 m wind speed (U10) and (b) relative humidity (RH) at 915 hPa for IRUN simulation. The dotted areas indicate statistical significance with 95% confidence from a two-tailed Student's *t* test. Differences between the total (Figure 1a) and the partial correlation coefficients explained by (c) U10 and (d) RH at 915 hPa.

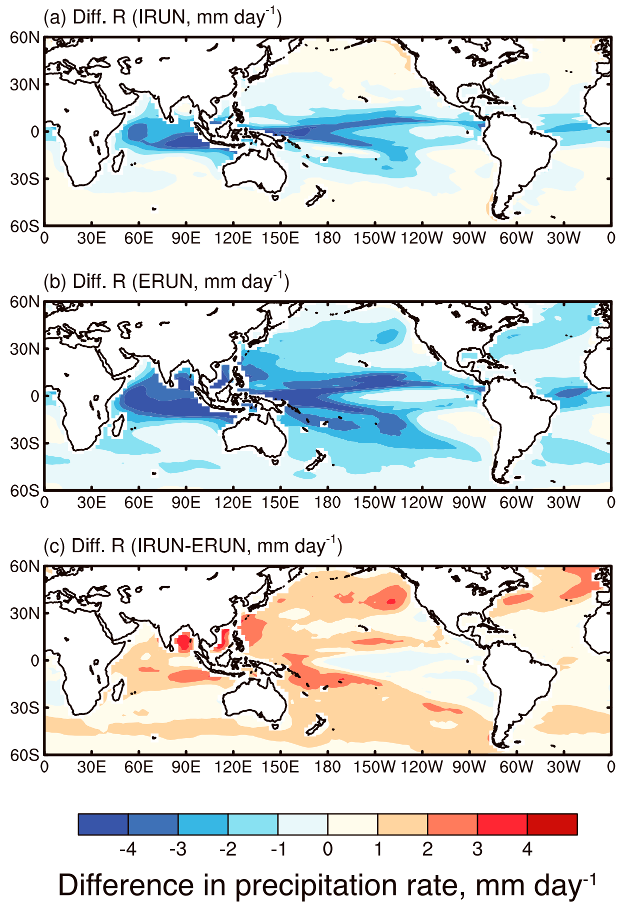

Figure 3. Composite differences in *R* between polluted and clean conditions (polluted-clean) for (a) IRUN and (b) ERUN, as well as (c) the changes in these differences between IRUN and ERUN. The clean and polluted conditions are defined as corresponding to the 33rd and 67th percentiles of the AOD for each grid box and simulations.

positive correlations between *R* and AOD (Figure 2c). The negative correlation coefficients over the tropical central-eastern Pacific Ocean are due to El Niño–Southern Oscillation events. During El Niño, sea-salt emissions are decreased due to reduced easterly winds in the lower atmosphere, whereas rainfall increases over the eastern Pacific. The correlation coefficients exhibit a small change when the contribution of RH is removed (Figures 2b and 2d), with the global area-weighted mean partial correlation coefficient of -0.04. These results demonstrate that the positive correlations of precipitation and AOD over the midlatitude oceans are mostly driven by wind speed. Further, its impact on *R*-AOD relationships is more important than the role of changes in relative humidity at 915 hPa.

To examine the causes of covariation of *R* and AOD with wind speed, we show in Figure S1 in the supporting information the correlation coefficients of AOD and *R* with U10 from a combination of satellite-retrieved and reanalysis data and IRUN simulation. Both observations and simulation show strong positive correlations between AOD and U10 over almost all the world oceans, resulting from the dominant contribution of sea-salt emissions to AOD in the clean remote regions [*Mulcahy et al.*, 2008; *Engström and Ekman*, 2010]. *R* and U10 also exhibit statistically significant positive correlations over the midlatitude oceans due to their meteorologically driven covariation. The positive correlations between AOD and U10 and between U10 and *R* lead to the positive relationships between *R* and AOD over the midlatitude oceans.

In order to quantify the magnitude of the covariation of *R* and AOD and compare with previous studies, Figure 3a shows the composite differences in *R* between polluted and clean conditions (polluted-clean) for the IRUN simulation, categorized by the 67th and 33rd percentiles of AOD. Relative to the clean conditions, the polluted conditions have lower *R* over the tropics and higher *R* over the midlatitude oceans, corresponding to the correlations between AOD and *R* (Figure 1a). The differences in *R* are +0.20, -1.13, and +0.38 mm d^{-1} averaged over the southern midlatitude, tropical, and northern midlatitude bands, respectively, and -0.56 mm d^{-1} averaged globally (Table 1). These differences in *R* also suggest negative *R*-AOD relationships over the tropics and positive relationships over the midlatitude oceans, in agreement with previous studies [*Boucher and Quaas*, 2013]. The wet scavenging dominates the relationships between *R* and AOD over the tropics, whereas these relationships are driven by other factors over the midlatitude oceans.

Figure 3b presents the composite differences in *R* between polluted and clean conditions for the ERUN simulation, in which simulation the role of wind speed is removed. The values of *R* are lower over almost all the world in the polluted conditions compared to the clean conditions, with the difference of -1.55 mm d^{-1} averaged globally. In contrast to the higher *R* over the midlatitude oceans during polluted conditions in IRUN, ERUN has lower *R*. This indicates that relationships between *R* and AOD are driven by covariation with wind speed.

Figure 3c shows the changes between IRUN and ERUN in composite differences in *R* contributed from the variations in wind speed. Variations in wind speed lead to increases in *R* over almost all the oceans between polluted and clean conditions, with increases by +1.01, +0.87, and +1.49 mm d^{-1} averaged over the southern midlatitude, tropical, and northern midlatitude bands, respectively (Table 1). The increase in *R* is +0.99 mm d^{-1} averaged globally, offsetting 64% of the decrease caused by wet scavenging between polluted and clean conditions.

To evaluate the impact of aerosol-cloud interactions in the relationships between *R* and AOD, we show in Figures S2a and S2b the composite differences in convective precipitation rate (R_{cnv}) and stratiform precipitation rate (R_{str}) between polluted and clean conditions, respectively. The differences in R_{cnv} are almost identical to those in *R* (sum of R_{cnv} and R_{str}), with global mean of -0.55 mm d^{-1}. Therefore, wet scavenging by convective precipitation dominates the relationships between *R* and AOD. The differences in R_{str} are much smaller than those in R_{cnv}, with a global mean value of -0.01 mm d^{-1} due to the smaller stratiform wet scavenging process over the tropics. Since the model only considers aerosol effects on stratiform cloud, such effects on relationships between *R* and AOD are much smaller than the covariation effects from other factors. But aerosol effects on convection are not considered in this model, which may cause some biases in the relationships.

Through evaluating relationships between *R* and dry AOD, *Boucher and Quaas* [2013] and *Grandey et al.* [2014] reported that covariation with relative humidity can explain a large component of the positive relationships between *R* and AOD. In this study, covariation with wind speed is also found to lead to the positive relationships over the midlatitude oceans. It is therefore of interest to compare the contributions of wind speed and relative humidity to the positive relationships between *R* and AOD. Because the model did not archive dry AOD in the output, which is an approximation of AOD without swelling hygroscopically, CCN concentrations at 0.1% supersaturation and 915 hPa are used here to represent dry AOD. Then polluted and clean conditions are defined as corresponding to the 67th and 33rd percentiles of the CCN. It should be noted that AODs (and dry AOD) are column measurements, whereas CCN at 915 hPa corresponds to a single pressure level, meaning that some differences between the metrics are to be expected. Figure S2c shows the composite differences in *R* between CCN-defined polluted and clean conditions for the IRUN simulation. These differences are similar in spatial patterns to those between AOD-defined polluted and clean conditions. However, these differences show more negative values, with a global mean difference of -1.00 mm d^{-1}. The variations in relative humidity lead to larger *R* in polluted conditions by +0.44 mm d^{-1} averaged globally, relative to those in clean conditions. This value is smaller than the +0.99 mm d^{-1} difference due to the variations in wind speed, indicating that the contribution of wind speed is larger than that of relative humidity to the relationships between *R* and AOD, consistent with the findings above using partial correlation analysis.

In order to compare our results with previous studies associated with *R*-AOD relationships, the correlation coefficients and composite differences are also calculated using daily data in June-July-August (JJA) for IRUN and ERUN and are shown in Figure S3. The result of positive relationships between *R* and AOD over the midlatitude oceans in IRUN changes to negative in ERUN, especially over southern midlatitude oceans, is the same as that using monthly anomaly data. The differences in *R* between polluted and clean conditions drop from -0.04 mm h^{-1} in IRUN to -0.14 mm h^{-1} in ERUN averaged globally. The variations in wind speed lead to larger *R* in polluted conditions by +0.10 mm h^{-1}, relative to those in clean conditions. This value is larger than +0.05 mm h^{-1}, the increase due to the variations in relative humidity calculated based on CCN for IRUN in this study, and also larger than +0.05 mm h^{-1}, the increase calculated based on dry AOD in *Grandey et al.* [2014]. This comparison also shows that the wind speed has a larger role than relative humidity in causing the positive correlations of *R* and AOD. It is worth mentioning that results in *Grandey et al.* [2014] include both land and ocean areas using ECHAM-HAM aerosol-climate model, and this study focuses on ocean areas using CESM-CAM5.

4. Conclusions

This study examines the relationships between aerosols and precipitation rate for all ocean regions between 60°S and 60°N using 150 year simulations in preindustrial conditions using CESM, satellite-retrieved and reanalysis data. Both simulation and observation show strong correlations between AOD and wind speed and between precipitation rate and wind speed. Through both partial correlation analysis and model simulations, wind speed is found to be one of the major drivers of precipitation-AOD relationships. The covariation with wind speed plays a large role in the relationships over the midlatitude oceans, which leads to the increases in precipitation in polluted conditions compared to clean conditions, defined according to percentiles of AOD. It offsets 64% of the wet scavenging-induced decrease in precipitation in polluted conditions globally. The wind speed is also found to have a larger impact than relative humidity at 915 hPa on the relationships between precipitation and AOD.

Aerosol effects on clouds and precipitation are still one of the largest uncertainties in the studies of climate. The results presented in this study highlight the influence of wind speed on the relationships between AOD and precipitation, which helps with interpretation of satellite data and better understanding of aerosol-cloud-precipitation relationships.

The results presented here are from CESM-CAM5, which only treats aerosol effects on stratiform cloud microphysics. Aerosol effects on convective clouds are neglected, which may cause biases. If future models would include aerosol effects on convective clouds, a more accurate aerosol-cloud-precipitation relationship could be presented.

Acknowledgments

This research was supported by National Science Foundation (NSF) AGS1048995 and by DOE DE-SC0006679 as part of the U.S. Department of Energy, Office of Science, Biological and Environmental Research, Decadal and Regional Climate Prediction using Earth System Models (EaSM) program. The Pacific Northwest National Laboratory is operated for the Department of Energy's (DOE) by Battelle Memorial Institute of Columbus, Ohio under contract DE-AC05-76RLO 1830. Observed 10 m wind speed data are obtained from the ERA-Interim reanalysis at the European Center for Medium Range Weather Forecasts (ECMWF). CMAP precipitation data are provided by the NOAA/OAR/ESRL PSD, Boulder, Colorado, USA, from their website at http://www.esrl.noaa.gov/psd/. This research used resources of the National Energy Research Scientific Computing Center, a DOE Office of Science User Facility supported by the Office of Science of the U.S. Department of Energy under contract DE-AC02-05CH11231. The data and codes for these results are posted at http://portal.nersc.gov/project/m1374/AOD_R.

References

Abdul-Razzak, H., and S. J. Ghan (2000), A parameterization of aerosol activation: 2. Multiple aerosol types, *J. Geophys. Res.*, *105*, 6837–6844, doi:10.1029/1999JD901161.

Ackerman, A. S. (2000), Reduction of tropical cloudiness by soot, *Science*, *288*(5468), 1042–1047, doi:10.1126/science.288.5468.1042.

Albrecht, B. (1989), Aerosols, cloud microphysics, and fractional cloudiness, *Science*, *245*, 1227–1230, doi:10.1126/science.245.4923.1227.

Boucher, O., and J. Quaas (2013), Water vapour affects both rain and aerosol optical depth, *Nat. Geosci.*, *6*(1), 4–5, doi:10.1038/ngeo1692.

Chand, D., R. Wood, S. J. Ghan, M. Wang, M. Ovchinnikov, P. J. Rasch, S. Miller, B. Schichtel, and T. Moore (2012), Aerosol optical depth increase in partly cloudy conditions, *J. Geophys. Res.*, *117*, D17207, doi:10.1029/2012JD017894.

Engström, A., and A. M. L. Ekman (2010), Impact of meteorological factors on the correlation between aerosol optical depth and cloud fraction, *Geophys. Res. Lett.*, *37*, L11814, doi:10.1029/2010GL044361.

Gettelman, A., X. Liu, S. J. Ghan, H. Morrison, S. Park, A. J. Conley, S. A. Klein, J. Boyle, D. L. Mitchell, and J.-L. F. Li (2010), Global simulations of ice nucleation and ice supersaturation with an improved cloud scheme in the Community Atmosphere Model, *J. Geophys. Res.*, *115*, D18216, doi:10.1029/2009JD013797.

Ghan, S. J., and R. A. Zaveri (2007), Parameterization of optical properties for hydrated internally mixed aerosol, *J. Geophys. Res.*, *112*, D10201, doi:10.1029/2006JD007927.

Grandey, B. S., P. Stier, R. G. Grainger, and T. M. Wagner (2013a), The contribution of the strength and structure of extratropical cyclones to observed cloud-aerosol relationships, *Atmos. Chem. Phys.*, *13*(21), 10,689–10,701, doi:10.5194/acp-13-10689-2013.

Grandey, B. S., P. Stier, and T. M. Wagner (2013b), Investigating relationships between aerosol optical depth and cloud fraction using satellite, aerosol reanalysis and general circulation model data, *Atmos. Chem. Phys.*, *13*(6), 3177–3184, doi:10.5194/acp-13-3177-2013.

Grandey, B. S., A. Gururaj, P. Stier, and T. M. Wagner (2014), Rainfall-aerosol relationships explained by wet scavenging and humidity, *Geophys. Res. Lett.*, *41*, 5678–5684, doi:10.1002/2014GL060958.

Gryspeerdt, E., P. Stier, and B. S. Grandey (2014), Cloud fraction mediates the aerosol optical depth-cloud top height relationship, *Geophys. Res. Lett.*, *41*, 3622–3627, doi:10.1002/2014GL059524.

Gryspeerdt, E., P. Stier, B. A. White, and Z. Kipling (2015), Wet scavenging limits the detection of aerosol effects on precipitation, *Atmos. Chem. Phys.*, *15*, 7557–7570, doi:10.5194/acp-15-7557-2015.

Haywood, J. M., V. Ramaswamy, and B. J. Soden (1999), Tropospheric aerosol climate forcing in clear-sky satellite observations over the oceans, *Science*, *283*, 1299–1303, doi:10.1126/science.283.5406.1299.

Hazewinkel, M. (Ed) (2002), *Encyclopaedia of Mathematics*, Springer, New York.

Hurrell, J. W., et al. (2013), The Community Earth System Model: A framework for collaborative research, *Bull. Am. Meteorol. Soc.*, *94*, 1339–1360, doi:10.1175/BAMS-D-12-00121.1.

Kaufman, Y. J., I. Koren, L. A. Remer, D. Rosenfeld, and Y. Rudich (2005), The effect of smoke, dust, and pollution aerosol on shallow cloud development over the Atlantic Ocean, *Proc. Natl. Acad. Sci. U.S.A.*, *102*, 11,207–11,212, doi:10.1073/pnas.0505191102.

Koren, I., Y. J. Kaufman, D. Rosenfeld, L. A. Remer, and Y. Rudich (2005), Aerosol invigoration and restructuring of Atlantic convective clouds, *Geophys. Res. Lett.*, *32*, L14828, doi:10.1029/2005GL023187.

Koren, I., L. A. Remer, Y. J. Kaufman, Y. Rudich, and J. V. Martins (2007), On the twilight zone between clouds and aerosols, *Geophys. Res. Lett.*, *34*, L08805, doi:10.1029/2007GL029253.

Koren, I., O. Altaratz, L. A. Remer, G. Feingold, J. V. Martins, and R. H. Heiblum (2012), Aerosol-induced intensification of rain from the tropics to the mid-latitudes, *Nat. Geosci.*, *5*(2), 118–122, doi:10.1038/ngeo1364.

Koren, I., G. Dagan, and O. Altaratz (2014), From aerosol-limited to invigoration of warm convective clouds, *Science*, *344*(6188), 1143–1146, doi:10.1126/science.1252595.

Lee, L. A., K. S. Carslaw, K. J. Pringle, and G. W. Mann (2012), Mapping the uncertainty in global CCN using emulation, *Atmos. Chem. Phys.*, *12*, 9739–9751, doi:10.5194/acp-12-9739-2012.

Liu, X., et al. (2012), Toward a minimal representation of aerosols in climate models: Description and evaluation in the Community Atmosphere Model CAM5, *Geosci. Model Dev.*, *5*, 709–739, doi:10.5194/gmd-5-709-2012.

Loeb, N. G., and G. L. Schuster (2008), An observational study of the relationship between cloud, aerosol and meteorology in broken low-level cloud conditions, *J. Geophys. Res.*, *113*, D14214, doi:10.1029/2007JD009763.

Lohmann, U., and J. Feichter (2005), Global indirect aerosol effects: A review, *Atmos. Chem. Phys.*, *5*, 715–737, doi:10.5194/acp-5-715-2005.
Mårtensson, E. M., E. D. Nilsson, G. de Leeuw, L. H. Cohen, and H.-C. Hansson (2003), Laboratory simulations and parameterization of the primary marine aerosol production, *J. Geophys. Res.*, *108*(D9), 4297, doi:10.1029/2002JD002263.
Mauger, G. S., and J. R. Norris (2007), Meteorological bias in satellite estimates of aerosol-cloud relationships, *Geophys. Res. Lett.*, *34*, L16824, doi:10.1029/2007GL029952.
Monahan, E. C., D. E. Spiel, and K. L. Davidson (1986), A model of marine aerosol generation via whitecaps and wave disruption, in *Oceanic Whitecaps*, edited by E. Monahan and G. M. Niocaill, pp. 167–174, D. Reidel, Norwell, Mass.
Morrison, H., and A. Gettelman (2008), A new two-moment bulk stratiform cloud microphysics scheme in the community atmosphere model, version 3 (CAM3). Part I: Description and numerical tests, *J. Clim.*, *21*(15), 3642–3659, doi:10.1175/2008jcli2105.1.
Mulcahy, J. P., C. D. O'Dowd, S. G. Jennings, and D. Ceburnis (2008), Significant enhancement of aerosol optical depth in marine air under high wind conditions, *Geophys. Res. Lett.*, *35*, L16810, doi:10.1029/2008GL034303.
Quaas, J., B. Stevens, P. Stier, and U. Lohmann (2010), Interpreting the cloud cover aerosol optical depth relationship found in satellite data using a general circulation model, *Atmos. Chem. Phys.*, *10*(13), 6129–6135, doi:10.5194/acp-10-6129-2010.
Rosenfeld, D., U. Lohmann, G. B. Raga, C. D. O'Dowd, M. Kulmala, S. Fuzzi, A. Reissell, and M. O. Andreae (2008), Flood or drought: How do aerosols affect precipitation? *Science*, *321*(5894), 1309–1313, doi:10.1126/science.1160606.
Smith R., et al. (2010), The Parallel Ocean Program (POP) reference manual, Tech. Rep. LAUR-10-01853, Los Alamos National Laboratory.
Stevens, B., and G. Feingold (2009), Untangling aerosol effects on clouds and precipitation in a buffered system, *Nature*, *461*(7264), 607–613, doi:10.1038/nature08281.
Su, W., G. L. Schuster, N. G. Loeb, R. R. Rogers, R. A. Ferrare, C. A. Hostetler, J. W. Hair, and M. D. Obland (2008), Aerosol and cloud interaction observed from high spectral resolution lidar data, *J. Geophys. Res.*, *113*, D24202, doi:10.1029/2008JD010588.
Twomey, S. (1977), The influence of pollution on the shortwave albedo of clouds, *J. Atmos. Sci.*, *34*, 1149–1152, doi:10.1175/1520-0469(1977)034<1149:TIOPOT>2.0.CO;2.